Tropomyosin Is Essential in Yeast, Yet the *TPM1* and *TPM2* Products Perform Distinct Functions

Beth Drees, Carol Brown,* Bart G. Barrell,* and Anthony Bretscher

Section of Biochemistry, Molecular and Cell Biology, Biotechnology Building, Cornell University, Ithaca, New York 14853; and *The Sanger Centre, Hinxton Hall, Hinxton, Cambridge CB10 1RQ, England

Abstract. Sequence analysis of chromosome IX of *Saccharomyces cerevisiae* revealed an open reading frame of 166 residues, designated *TPM2*, having 64.5% sequence identity to *TPM1*, that encodes the major form of tropomyosin in yeast. Purification and characterization of Tpm2p revealed a protein with the characteristics of a bona fide tropomyosin; it is present in vivo at about one sixth the abundance of Tpm1p. Biochemical and sequence analysis indicates that Tpm2p spans four actin monomers along a filament, whereas Tpm1p spans five. Despite its shorter length, Tpm2p can compete with Tpm1p for binding to F-actin. Over-expression of Tpm2p in vivo alters the axial budding of haploids to a bipolar pattern, and this can be partially suppressed by co-over-expression of Tpm1p. This suggests distinct functions for the two tropomyosins, and indicates that the ratio between them is important for correct morphogenesis. Loss of Tpm2p has no detectable phenotype in otherwise wild type cells, but is lethal in combination with *tpm1*Δ. Over-expression of Tpm2p does not suppress the growth or cell surface targeting defects associated with *tpm1*Δ, so the two tropomyosins must perform an essential function, yet are not functionally interchangeable. *S. cerevisiae* therefore provides a simple system for the study of two tropomyosins having distinct yet overlapping functions.

TROPOMYOSINS are integral components of the actin-based contractile apparatus and actin-based cytoskeleton of muscle and non-muscle cells. All tropomyosins are highly α-helical coiled-coil dimers that bind head-to-tail along the actin filament (reviewed by Payne and Rudnick, 1985). In striated muscle, tropomyosin together with troponin confers Ca^{2+}-dependent regulation of the actin-myosin interaction (Ebashi et al., 1972), whereas in smooth muscle the association of tropomyosin with caldesmon is believed to be involved in thin filament contraction (Bretscher, 1986). Multiple isoforms of tropomyosins are also found in vertebrate non-muscle cells (Cote, 1983; Lin et al., 1985; Matsumara and Yamashiro-Matsumara, 1985). This diversity is generated by the expression of different genes as well as by alternative splicing of their transcripts (Helfman et al., 1986; reviewed by Breitbart et al., 1987). These isoforms differ in size, from the 284 residues typical of muscle tropomyosins, to 248 residues (or 247 after processing [Cote, 1983]) which are the most abundant in non-muscle cells. The various tropomyosins in non-muscle cells have different actin-binding activities, vary in their expression between tissues, and show different intracellular localizations (Lin et al, 1985; Matsumara and Yamashiro-Matsumara, 1985; Broschat and Burgess, 1986; Lin et al., 1988; Pittenger and Helfman, 1992). Transformation by oncogenic viruses affects isoform expression at the transcriptional level, with the longer isoforms being reduced in favor of increased expression of the shorter forms. These changes accompany alterations in cell morphology (Hendricks and Weintraub, 1981; Matsumara et al, 1983; Lin et al., 1985; Cooper et al., 1985). Despite the clear importance of tropomyosins, the distinct contributions of the various isoforms have been difficult to ascertain.

The budding yeast *Saccharomyces cerevisiae* has become a popular organism for studying basic cellular processes, including those involving the F-actin cytoskeleton. In spite of its small genome size and evolutionary distance from multicellular eukaryotic cells, the similarity in the functional organization of the microfilament based cytoskeleton from yeast to man is remarkable (for review see Bretscher et al, 1994; Welch et al., 1994). In yeast, actin shows a cell cycle–regulated distribution that implies a role in the delivery of materials to the cell surface for polarized growth. Actin filaments are found in two distinct locations: bundles of filaments ("cables") extend from the mother into the bud, and actin filaments are associated with cortical structures that are likely to be the sites of cell surface growth. Many components of the yeast microfilament cytoskeleton have been identified and the consequences of loss of these components explored. One of these components is tropomyosin.

The major form of tropomyosin in budding yeast is the

Address all correspondence to A. Bretscher, Section of Biochemistry, Molecular and Cell Biology, Cornell University, 351 Biotechnology Bldg., Ithaca, NY 14852. Ph.: (607) 255-5713. Fax: (607) 255-2428.

product of the *TPM1* gene. Biochemical and structural characterization revealed that Tpm1p has many features in common with higher cell tropomyosins, including heat stability, acidic isoelectric point, and cooperative, saturable cation-dependent binding to F-actin (Liu and Bretscher, 1989*a*). The predicted product of the *TPM1* gene is 199 residues in length, has sequence characteristics of a coiled-coil protein and shows 20% identity to higher cell tropomyosins. Immunolocalization reveals that Tpm1p selectively associates with actin cables in yeast, but is not enriched in the cortical patches that are probably the sites of cell surface growth (Liu and Bretscher, 1989*b*; Mulholland et al, 1994). Loss of Tpm1p results in viable, but unhealthy cells, which lack actin cables, suggesting that Tpm1p is important for the stability of actin cables, and randomized cortical structures. Two lines of evidence suggest that Tpm1p is important for polarized transport of vesicular material for cell surface growth in yeast. First, phenotypic analysis of cells lacking Tpm1p reveals partial defects in polarized delivery to the cell surface, in mating projection formation, in cell fusion during mating, and the abnormal accumulation of intracellular vesicles. Second, genetic data indicate that Tpm1p and the double-headed non-filamentous myosin encoded by *MYO2* function in the same pathway, which in the case of Myo2p has also been suggested to be in vesicular transport (Johnston et al., 1991). Additional genetic data involving combinations of conditional mutations in *SEC* genes with *tpm1*Δ suggest that the vesicular accumulation phenotype of strains harboring *tpm1*Δ is due to a post-Golgi defect (Liu and Bretscher, 1992).

Here we describe the presence of a gene, designated *TPM2*, that encodes a second tropomyosin in yeast. Characterization of the purified Tpm2p and analysis of disruptions of the *TPM2* gene indicate that it performs a distinct function from Tpm1p, but that together *TPM1* and *TPM2* perform an essential function.

Materials and Methods

Plasmid and Strain Construction

All PCR products were initially recovered using the TA cloning kit (Invitrogen, San Diego, CA). The strain DH5α was used for all manipulations involving *Escherichia coli*. The lithium acetate method was used for all yeast transformations (Ito et al., 1983). The *S. cerevisiae* strains used in this study are listed in Table I.

Construction of pBD100: GAL1-TPM1 Overexpression Plasmid

The Tpm1p overexpression plasmid previously described (Liu and Bretscher, 1989*b*) contains the *GAL10-GAL1* promoter region and the *TPM1* gene including 219 bases of upstream coding region. In this construct, Tpm1p is not under tight transcriptional control of the *GAL1* promoter. A construct which allowed controlled expression of Tpm1p was created by exonuclease III treatment of this plasmid to remove bases −171 to −18 of the *TPM1* upstream flanking region. When this plasmid (pBD100) was introduced into a *tpm1*Δ strain and grown on minimal media containing glucose, no detectable Tpm1p was produced and there was no suppression of the *tpm1*Δ-associated defects.

Construction of pBD101: GAL1-TPM2 Overexpression Plasmid

The *GAL10-GAL1* promoter region from YCp50-Sc4816ΔAUG (Goff et al., 1984) was cloned into the EcoRI-BamHI sites of 2 μ-based plasmid YEp352, as described in a previous paper (Hill et al., 1986; Liu and Bretscher, 1989*b*). The *TPM2* gene was amplified using PCR, using primers which introduced a SalI site −4-bases upstream of the start codon and a HindIII site 468-bases downstream of the stop codon. PCR amplification using genomic DNA from the wild type diploid ABY173 as template produced a fragment of about 970 bases. This was cloned into the SalI-HindIII sites behind the *GAL1* promoter to generate plasmid pBD101. The authenticity of *TPM2* was confirmed by DNA sequence analysis.

Construction of pBD103: a Vector for tpm2Δ::HIS3 Disruption

Genomic DNA prepared from the wild type diploid strain ABY173 was used as the template for PCR amplification. The *TPM2* gene (486-bp open reading frame) was amplified using a primer with homology to the 5′ flanking sequence which had been engineered to insert a BamHI site 242-bases upstream of the start codon and a primer with homology to the 3′ flanking sequence which introduced a HindIII site 482-bases downstream from the stop codon. PCR amplification produced a product of about 1.2 kb. The 1.2-kb BamHI-HindIII fragment was cloned into pUC13. A 1.8-kb fragment containing the *HIS3* marker was inserted into the *TPM2* gene at the unique BglII site at position 232 in the open reading frame. EcoRI digestion produces a fragment which contains the intervening *HIS3* marker, flanked by 381 bases of 5′ flanking sequence and *TPM2* NH_2-terminal coding region on one side, and by 183 bases of *TPM2* COOH-terminal coding region on the other. The linear DNA was transformed into wildtype diploids (ABY173) and His^+ transformants were isolated. The diploids were sporulated and gave rise to four viable spores. His^+ haploids did not contain detectable Tpm2p and therefore contained a disrupted *TPM2* gene.

Construction of pBD104: A Vector for tpm2Δ::URA3 Disruption

PCR amplification was used to obtain a 229-bp fragment of 5′ flanking sequence using primers which insert a BamHI site at position −232 and a SalI site at position −23 upstream from the *TPM2* start codon. This fragment was cloned into the BamHI-SalI sites in the Ylp5 plasmid. A EcoRI-HindIII fragment containing 71 bases of *TPM2* COOH-terminal coding region and 482 bases of 3′ flanking region was cloned into the same construct. Digestion of this plasmid with BamHI and HindIII produces a linear DNA which contains 229 bases of *TPM2* 5′ sequence. Ylp5 plasmid DNA containing the *URA3* selectable marker, and 553 bases including part of the COOH-terminal coding region and 3′ flanking sequence. The linear DNA was introduced into a wild type haploid strain and Ura^+ transformants were isolated. Alternatively, the plasmid was introduced into the diploid (ABY173) which was then sporulated. Four viable spores were recovered, two of which were Ura^+ and lacked detectable Tpm2p.

Purification of Tpm2p

Cells (ABY432), lacking Tpm1p and carrying the *GAL1-TPM2* plasmid pBD101, were grown to early log phase in minimal media with galactose. The cells were harvested, washed, resuspended in extraction buffer (0.3 M KCl, 0.5 mM $MgCL_2$, 50 mM Imidazole/HCl, pH 6.9, 0.3 mM phenylmethylsulfonyl fluoride), and lysed by passage through a French press at 15,000 p.s.i. Cell lysate was boiled for 10–20 min and then centrifuged at 12,000 *g* for 20 min to allow recovery of heat stable, soluble proteins. Ammonium sulfate was added to the supernatant to give 40% saturation and then centrifuged to remove the precipitate. The ammonium sulfate concentration was increased to 80% saturation and the precipitated material recovered by centrifugation at 12,000 *g* for 20 min. The resulting pellet was resuspended in a minimal volume, and dialyzed into 0.2 M KCl, 10 mM KH_2PO_4-K_2HPO_4, pH 7.0, 1 mM DTT. The material was clarified by centrifugation and applied to a 10 ml Q-Sepharose anion exchange column. The column was washed with 50 ml of buffer, and then developed with a 100 ml gradient from 0.2 to 1 M KCl. Peak fractions of the 25-kD heat stable protein eluted at about 0.4 M KCl. Fractions containing pure Tpm2p were obtained in this manner. These fractions were dialyzed into distilled water, and aliquots were frozen and lyophilized to allow preparation of concentrated stock solutions. Approximately 2.8 mg of Tpm2p was obtained from a starting weight of 10 g wet, washed cells.

Estimation of the Relative Abundance of Tpm1p and Tpm2p

To estimate the relative abundance of each tropomyosin, an enriched heat

Table I. Yeast Strains Used in This Study

Strain	Genotype*	Source
CUY25	*MATa, ade2-101, his3-Δ200, leu2-3,112, ura3-52*	T. Huffaker (Cornell University, Ithaca NY)
CUY28	*MATα, ura3-52, his3-Δ200, leu2-3,112, lys2-801, trp1-1(am)*	T. Huffaker
CUY29	*MATα, GAL⁺, ura3-52, his3-Δ200, leu2-3,112*	T. Huffaker
CUY30	*MATa, GAL⁺, ura3-52, his3-Δ200, leu2-3,112, lys2-801, ade2-101*	T. Huffaker
ABY107	*MATa, leu2-3,112; ura3-52, abp1Δ::URA3*	Drubin et al., 1988
ABY110	*Matα, ura3-52, his3-Δ200, leu2-3,112, trp1-1(am), sac6Δ::URA3*	Adams et al., 1991
ABY117	*Mata, leu2-3,112, ura3-52, his3Δ200, ade2-101, trp1-1(am), myo2-66*	Johnston et al., 1991
ABY173	CUY25 × CUY28	
ABY167	*MATα, GAL⁺, ura3-52, his3-Δ200, leu2-3,112; lys2-801, ade2-101, tpm1Δ::LEU2*	Liu and Bretscher, 1989*b*
ABY187	*Matα, ura3-52, his3-Δ200, leu2-3,112, ade2-101, trp1-1(am), myo1Δ::LEU2*	Watts et al., 1987
ABY230	CUY30 background, *MATa* (YCp50-HO plasmid mediated mating type switch, Russell et al., 1986), *tpm1Δ::LEU2.*	This study
ABY430	*Matα, leu2-3,112, ura3-52, his3Δ200, mys2-801, trp1-1(am), myo4Δ::URA3*	Haarer et al., 1994
ABY431	CUY29 [pBD101]	This study
ABY432	ABY230 [pBD101]	This study
ABY433	CUY29 [pBD100]	This study
ABY434	CU29 [pBD100, pBD102]	This study
ABY435	ABY173, *tpm2Δ::HIS3/+*	This study
ABY436	ABY 435 segregant, *MATa, ura3-52, his3-Δ200, leu2-3,112, lys2-801, ade2-101, trp1-1(am), tpm2Δ::HIS3*	This study
ABY439	ABY435 segregant, *MATα, ura3-52, his3-Δ200, leu2-3,112, lys2-801, tpm2Δ::HIS3*	This study
ABY440	ABY435 segregant, *MATα, ura3-52, his3-Δ200, leu2-3,112, lys2-801*	This study
ABY441	CUY29, *tpm2Δ::URA3*	This study
ABY442	ABY167 × ABY436	This study
ABY443	ABY173, *tpm2Δ::URA3/+*	This study

* The presence of multicopy plasmids is indicated in square brackets, whose construction is described in Materials and Methods.

stable lysate of wild type cells was prepared and the abundance of the isoforms determined by densitometry of Coomassie blue-stained SDS gels. Wild type diploid (ABY173) was grown to late exponential phase in rich medium, harvested, washed and resuspended in extraction buffer (see above). 50 g of cells were lysed by passage through a French press and boiled. The heat stable soluble fraction was dialyzed against 0.1 M KCl in the same buffer and loaded on a 10 ml Q-Sepharose column. After washing with the same buffer, bound proteins were eluted with 1 M KCl. This enriched fraction contains all the Tpm1p and Tpm2p and removes some other species that comigrate with these proteins in total heat stable lysates. The identity of the Tpm1p and Tpm2p polypeptides was determined in heat stable lysates of strains lacking these proteins.

Biochemical and Physical Characterization of Tpm2p

Oxidative cross-linking of Tpm2p was performed as described (Stewart, 1975). Stokes radius values for Tpm1p and Tpm2p were determined using a Sepharose S-300 gel filtration column calibrated with BSA, ovalbumin, aldolase, and myoglobin. The sedimentation coefficient of Tpm2p was determined by sucrose gradient ultracentrifugation with BSA, ovalbumin, and myoglobin standards (Bretscher, 1984). Matrix-assisted laser desorption mass spectroscopy of Tpm2p was performed on HPLC-purified Tpm2p as described (Wang and Chait, 1994).

F-Actin Cosedimentation Assays

Cosedimentation assays were performed using rabbit skeletal muscle F-actin (Bretscher, 1984) and purified Tpm1p or Tpm2p. All proteins were dialyzed into 100 mM KCl, 0.5 mM $MgCl_2$, 1 mM DTT, 2 mM ATP, 5 mM Tris-HCl, pH 7.6. For determination of Mg^{2+} and KCl effects on binding, 2 μM actin and 1.3 μM dimeric Tpm2p were used in each binding reaction. Saturation binding of Tpm1p and Tpm2p to F-actin was carried out using increasing concentrations of either Tpm1p or Tpm2p and F-actin, at 10 mM $MgCl_2$ and 30 mM KCl. To determine the effects of Tpm1p and Tpm2p on each others' binding behavior, assays were performed using subsaturating ratios of tropomyosin to F-actin (2 μM actin, 0.4 μM Tpm1p, 0.5 μM Tpm2p), with addition of increasing amounts of the other tropomyosin. 100-μl samples were mixed in micro-ultracentrifuge tubes for 30 min at room temperature, and then centrifuged at 125,000 *g* for 20 min in a Beckman TL100 ultracentrifuge to pellet F-actin and associated protein. Pellet and supernatant fractions were analyzed by SDS-PAGE and the ratio of tropomyosin bound to F-actin in the pellet fraction was determined by densitometry of Coomassie-stained gels.

Genetic Techniques

The effect of combining *tpm2Δ::HIS3* with mutations in other yeast cytoskeletal genes (*abp1Δ::URA3, sac6Δ::URA3 myo1Δ::LEU2, myo2-66, myo4Δ::LEU2, tpm1Δ::LEU2*) was determined by setting up crosses to produce diploids heterozygous for both mutant alleles. These were sporulated and dissected, and segregation of marker genes, or, in the case of *myo2-66*, temperature sensitivity, was used for analysis of the products of each cross. In each cross, except between *tpm1Δ* and *tpm2Δ*, approximately equal numbers of viable parental and non-parental ditypes were recovered. A plasmid loss experiment was used to confirm the synthetic lethality produced by the combination of *tpm2Δ::HIS3* and *tpm1Δ::LEU2* alleles by introducing either the *GAL1-TPM1* or *GAL1-TPM2* multicopy plasmids (pBD100, pBD101) into the heterozygous diploid strain ABY442, which was sporulated and dissected. Leu⁺, His⁺, Ura⁺ haploid isolates were recovered and tested for their ability to grow on 5-fluoroorotic acid (5-FOA)[1] to determine if they could grow in the absence of the *URA3*-containing plasmid. Haploids which carried both the *LEU2* and *HIS3* markers, indicating that both *TPM1* and *TPM2* genes were disrupted, were unable to grown on 5-FOA.

Tpm2p Over-expression Studies and Fluorescence Techniques

The *GAL1-TPM2* multicopy plasmid (pBD101) was introduced into wild type and *tpm1Δ::LEU2* cells to generate strains ABY431 and ABY432. Transformants were grown in minimal media plus galactose to determine the effect of Tpm2p over-expression. Cultures were grown to early log phase and fixed

1. *Abbreviation used in this paper*: 5-FOA, 5-fluoroorotic acid.

in 3.7% formaldehyde for 1 h at room temperature. Cells were washed, resuspended at a concentration of 2×10^8 cells/ml, and incubated at 4°C in PBS containing 20 U/ml rhodamine-phalloidin (Molecular Probes, Inc., Eugene, OR) to allow visualization of the F-actin cytoskeleton by fluorescence microscopy. Chitinous bud scars were visualized by staining with Calcofluor (Fluorescent Brightener 28; Sigma Chemical Co., St. Louis, MO) at a concentration of 0.2 mg/ml. Cells were examined in a Zeiss Axioskop fluorescence microscope equipped for Nomarski and epifluorescence. Images were recorded on T-MAX 400 film.

Immunological Techniques

Rabbit polyclonal antisera was raised against purified Tpm2p. The crude antisera showed significant cross-reactivity with Tpm1p.

Results

TPM2 Encodes a Protein with Homology to the TPM1 Gene Product and the Sequence Characteristics of a Tropomyosin

Sequencing of yeast chromosome IX revealed an open reading frame which encodes a protein with significant sequence homology to the *TPM1* gene product. As this is the second tropomyosin gene to be discovered in *S. cerevisiae*, we have designated it *TPM2*.

The *TPM2* gene encodes a 161-residue protein (Fig. 1) whose sequence contains seven amino acid heptad pseudorepeats typically having hydrophobic residues at the first and fourth position in each repeat, a feature characteristic of an α-helical coiled-coil dimer (Stone and Smillie, 1978). When the sequences of the *TPM1* and *TPM2* gene products are aligned they show 64.5% overall sequence identity. A unique feature of the 199-residue *TPM1* gene product is the presence of two 38-amino acid pseudorepeating regions, found in residues 31–69 and 70–108, which show about 85% sequence identity. When *TPM1* and *TPM2* are aligned for maximum homology, the NH_2 and COOH termini show perfect alignment with an internal deletion in *TPM2* that precisely coincides with one of the pseudorepeats in *TPM1* (Fig. 1).

Expression and Purification of Tpm2p

Primers with homologies in the 5′ and 3′ flanking regions of the gene were generated and used to clone the *TPM2* gene by PCR amplification from genomic DNA. Sequencing of the cloned PCR product verified that it was the correct *TPM2* sequence.

In order to allow high-yield production of Tpm2p protein for easier purification, *TPM2* was placed under the control of the *GAL1* promoter (Fig. 2 *A*). The *GAL1-TPM2* fusion was constructed on a multicopy plasmid and introduced into a *tpm1Δ::LEU2* haploid yeast strain. Cells were grown in minimal media in glucose, or in galactose to induce high-level expression of Tpm2p. Since all known tropomyosins remain soluble in crude cell extracts after the bulk of the proteins have been precipitated by heating to 95°C, the heat-soluble proteins in these cells were examined after growth in glucose or in galactose. Gel electrophoresis revealed a heat stable protein with an apparent molecular mass of 25 kD in the cells grown in galactose but not in glucose (Fig. 2 *B*).

Purification of the 25-kD protein was carried out using a *tpm1Δ::LEU2* haploid strain carrying the *GAL1-TPM2* construct on a multicopy plasmid to eliminate the co-purification of Tpm1p. It was purified using a variation of the protocol developed for Tpm1p purification, which itself is based on typical methods for the isolation of nonmuscle tropomyosins (Cote and Smillie, 1981*a*; Liu and Bretscher, 1989*a*). In outline, a heat stable, soluble cell lysate was prepared from cells grown in minimal media with galactose. This was fractionated by ammonium sulfate precipitation and Q-Sepharose anion exchange column chromatography. A homogeneous preparation of Tpm2p was obtained (Fig. 2 *B*, lane *3*).

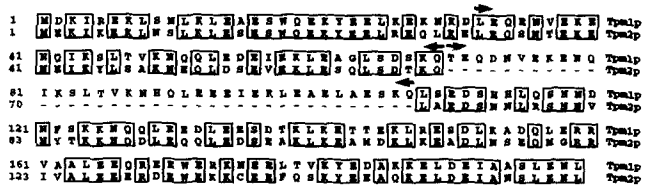

Figure 1. Alignment of the *TPM1* and *TPM2* gene products. When the two sequences are aligned for maximal homology, they are 64.5% identical. Tpm2p lacks one of the two amino acid pseudorepeating regions found in Tpm1p, which are indicated by sets of arrows. The *TPM2* sequence is available from Genbank/EMBL/DDBJ under accession number Z38059.

Biochemical and Physical Properties of Tpm2p

Biochemical and physical properties of Tpm2p were determined, and are compared to those of Tpm1p and platelet tropomyosin in Table II. The molecular mass of monomeric Tpm2p was determined by mass spectroscopy and found to be 19,115 D, which is within experimental error of the predicted value of 19,127 D. Like other tropomyosins, the 25-kD apparent molecular weight of Tpm2p determined by gel electrophoresis is higher than that predicted by the amino acid sequence of the protein.

Tropomyosins exist as dimers of two parallel α-helices in coiled-coil chains. Catalyzed air oxidation of cysteine residues has been used to show that the two polypeptide chains in the dimer are in register (Stewart, 1975). Tpm2p contains a single cysteine residue at position 137 in the amino acid sequence and air oxidation generated the expected dimeric

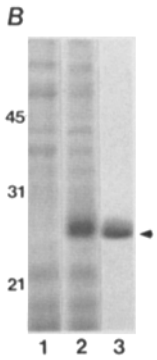

Figure 2. (*A*) *GAL1-TPM2* expression construct. This construct was made in a multicopy plasmid (pBD101) and introduced into *tpm1Δ* (ABY-432) cells. (*B*) Expression and purification of Tpm2p. *Lane 1*, SDS-PAGE of heat stable soluble protein from cells grown in glucose; lane *2*, cells grown in galactose; lane *3*, Q-Sepharose peak fraction containing pure Tpm2p.

Table II. Comparison of the Physical Properties of Yeast Tropomyosins with Equine Platelet Tropomyosin

	Tpm1p*	Tpm2p	Platelet TM‖
Apparent subunit mol wt	33 kD	25 kD§	30 kD
Isoelectric point	4.5	4.4‡	4.3
Sedimentation coefficient	2.6 S	2.4 S¶	2.7 S
Stokes radius	5.7 nm	5.2 nm¶	NR

* Liu and Bretscher, 1989*a*.
‡ Cote and Smillie, 1981*a*.
§ Apparent subunit molecular weight determined by SDS-PAGE.
‖ Isoelectric point of Tpm2p calculated from predicted protein sequence.
¶ Sedimentation coefficient and Stokes radius determined as described.
NR, not reported.

species as determined by gel electrophoresis under nonreducing conditions (not shown). Therefore, Tpm2p probably exists as a dimer with the chains in register, as expected.

Further characterization of Tpm2p included the determination of its apparent Stokes radius (5.2 nm) by gel filtration and sedimentation coefficient (2.4 *S*) in sucrose velocity gradients. The isoelectric point predicted for the protein encoded by the *TPM2* open reading frame is 4.4, a value typical for tropomyosins. These values are all consistent with the Tpm2p being an elongated coiled-coil dimeric protein.

Characterization of the Interaction of Tpm2p with F-actin

A defining characteristic of tropomyosins is their cation-dependent binding to F-actin. To examine the ability of Tpm2p to bind F-actin, cosedimentation assays with F-actin under various conditions were performed. Tpm2p exhibits Mg^{2+} dependent F-actin binding, with optimal binding at $\geq$2 mM $MgCl_2$ (Fig. 3 *A*). This Mg^{2+} dependent binding profile is very similar to that obtained for Tpm1p and other nonmuscle tropomyosins (Cote and Smillie, 1981*b*; Fowler and Bennett, 1984; Matsumara and Yamashiro-Matsumara, 1985; Liu and Bretscher, 1989*a*).

The effect of ionic strength on the interaction of Tpm2p with F-actin was also determined using cosedimentation assays performed in 10 mM $MgCl_2$ and at differing concentrations of KCl (Fig. 3 *B*). Tpm2p binding to actin was reduced with increasing salt concentrations, but with a profile quite distinct from that seen for Tpm1p. Tpm1p binding to F-actin is nearly abolished at 300 mM KCl (Liu and Bretscher, 1989*a*), whereas under the same conditions an appreciable amount of Tpm2p can bind to F-actin.

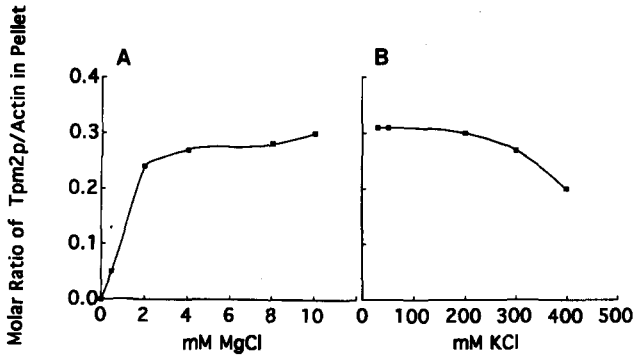

Figure 3. Effect of Mg^{2+} (*A*) and KCl (*B*) on Tpm2p interaction with F-actin. Binding was measured using F-actin cosedimentation assays. Results are expressed as molar ratio of Tpm2p dimers to actin monomers as determined by densitometry of stained SDS-PAGE of F-actin containing pellets.

The ratio of tropomyosin to F-actin at saturation was determined for both Tpm2p and Tpm1p under conditions optimal for the binding of both tropomyosins (10 mM $MgCl_2$, 30 mM KCl). Ratios of tropomyosin bound to actin in the pellet fraction were determined by densitometry of stained gels. The molar ratio of Tpm1p dimers to actin monomers at saturation binding was 0.215, or approximately one Tpm1p dimer to 4.6 actin monomers. The molar ratio of Tpm2p dimers to actin monomers at saturation was 0.27, or approximately one Tpm2p dimer to 3.6 actin monomers.

Tpm1p and Tpm2p Influence Each Other's Actin Binding Behavior In Vitro

To determine if Tpm1p and Tpm2p could influence each other's F-actin binding behavior, cosedimentation assays were carried out using both proteins. In these experiments, the level of one protein was held constant, and increasing amounts of the other protein were added. All reactions were carried out at subsaturating ratios of tropomyosin to F-actin and at concentrations of 30 mM KCl and 10 mM $MgCl_2$.

Addition of Tpm1p had little effect on the ability of Tpm2p to bind F-actin (Fig. 4 *A*). In contrast, addition of increasing levels of Tpm2p to reactions containing Tpm1p and F-actin showed that Tpm2p had a negative effect on Tpm1p binding to F-actin (Fig. 4 *B*). The molar ratio of Tpm1p bound to actin decreased steadily as Tpm2p was added in increasing amounts. Our results suggested that the binding of Tpm2p might be enhanced at low levels of Tpm1p (Fig. 4 *A*). We

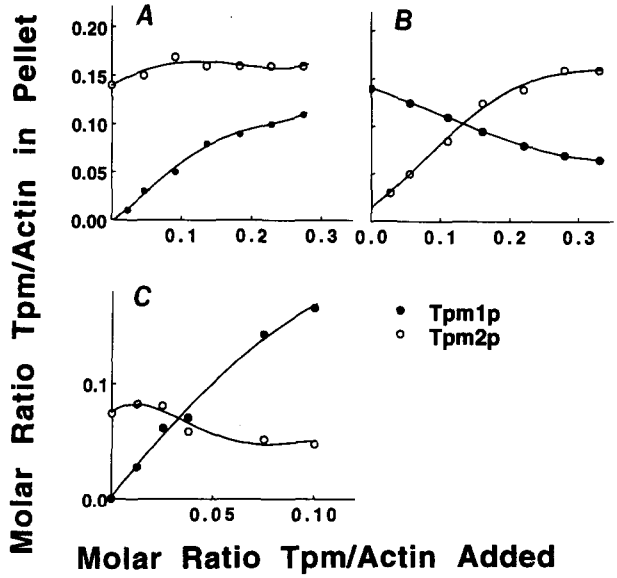

Figure 4. Competition binding assays of Tpm1p and Tpm2p to F-actin. (*A*) Effect of increasing Tpm1p concentration on Tpm2p binding to F-actin. (*B*) Effect of increasing Tpm2p concentration on Tpm1p binding to F-actin. (*C*) Amplification of the slight cooperative effect which increasing Tpm1p has on Tpm2p binding to actin. Results are expressed as molar ratios of tropomyosin dimers to actin monomers as determined by densitometry of stained SDS-PAGE of F-actin containing pellets.

therefore tried to examine this effect further by using a lower initial ratio of Tpm2p to F-actin in order to amplify any cooperative effect on Tpm2p binding produced by addition of Tpm1p (Fig. 4 *C*). Under these conditions there was a reproducible small degree of cooperativity, but it was not a major effect. Thus, under the conditions of our studies, Tpm2p competes with Tpm1p binding to F-actin, suggesting that its interaction with the actin filament is stronger. These results demonstrate that Tpm1p and Tpm2p are able to inhabit the same actin filament and to influence each other's actin binding behavior in vitro.

TPM2 Is a Not an Essential Gene

A 1.2-kb fragment containing the *TPM2* gene and its surrounding 5′ and 3′ flanking sequences was amplified by PCR from genomic DNA using primers which introduced a BamHI site 252-bases upstream of the start codon and a HindIII site 482-bases downstream of the stop codon. A construct for disruption of *TPM2* was generated by insertion of the *HIS3* cassette at the unique BglI site at position 237 in the open reading frame of the gene (Fig. 5 *A*). This linear fragment was introduced into a wild type diploid strain.

His$^+$ diploids were isolated, sporulated, and dissected to determine if disruption of the *TPM2* gene produced any phenotypic effects. Dissection produced four viable segregants, with the *HIS3* marker segregating 2:2. Immunoblots using polyclonal antiserum raised against purified Tpm2p demonstrated that Tpm2p was absent in heat stable cell lysates prepared from haploid His$^+$ segregants from this cross (Fig. 5 *C*), revealing that the gene disruption was successful and that *TPM2* is not an essential gene. Cells carrying the *tpm2Δ::HIS3* disruption were indistinguishable from wild type cells in their growth rate on solid and in liquid media at 30°C, in their morphology, in their budding pattern as determined by Calcofluor staining, in their actin cytoskeleton as determined after rhodamine–phalloidin staining, in their osmotic sensitivity as judged by growth on YPD containing 0.6 M NaCl or their mating efficiency.

Since the *tpm2Δ::HIS3* disruption still had 232 bases of intact NH_2-terminal coding sequence, it was possible that a truncated version of the *TPM2* gene product was being produced and was sufficient to mask any phenotypic effects which might result from total loss of the gene product. To verify that this was not the case, a second construct was used to replace the entire gene with the *URA3* marker. Disruption of the *TPM2* gene using this construct deletes all but the last 68 bases of *TPM2* coding region (Fig. 5 *B*). This construct was successfully introduced into a wild type haploid (CUY29) or diploid (ABY173) strain. Ura$^+$ haploids, generated by direct transformation or after sporulation of the diploid, were found to lack Tpm2p by immunoblot analysis of the heat stable cell lysates. These *tpm2Δ::URA3* deletions also failed to generate any obvious phenotype.

With the availability of strains that specifically lacked Tpm1p or Tpm2p, we were able to unambiguously identify the polypeptides in heat stable lysates that were the products of the *TPM1* and *TPM2* genes. Densitometry of Coomassie blue–stained gels of enriched heat stable lysates of exponentially growing wild type cells indicated that Tpm1p is about six times more abundant that Tpm2p.

Genetic Interaction of tpm2Δ with tpm1Δ and Mutations in Other Genes Encoding Cytoskeletal Proteins

To explore whether the *TPM2* gene product functions with other components of the cytoskeleton, the effect of combining *tpm2Δ::HIS3* with other cytoskeletal mutations was investigated. *tpm2Δ::HIS3* haploid strains of appropriate mating type (ABY436 or ABY439) were crossed with *sac6Δ::URA3*, *abp1Δ::URA3*, *myo1Δ::LEU2*, *myo2-66*, and *myo4Δ::LEU2* haploids (Watts et al., 1987; Drubin et al., 1988; Adams et al., 1991; Johnston et al., 1991; Haarer et al., 1994). Diploids were isolated, sporulated, and dissected. In each of these cases non-parental ditypes were recovered, and four viable spores were obtained in each case, indicating that *TPM2* does not show any synthetic lethal interaction with these genes.

The *tpm2Δ* strain was also crossed to *tpm1Δ* strain for the same type of analysis. Diploids were sporulated and dissected. Out of 19 tetrads dissected, four parental ditypes, four non-parental ditypes and eleven tetratypes were recovered. All haploids isolated from this cross were viable except for those that carried both the *LEU2* and *HIS3* markers, indicating that the *tpm2Δ/tpm1Δ* combination is lethal. Microscopic examination of plates on which spores from this cross had been dissected revealed small clusters of four to eight cells, indicating that the defect is not in sporulation, but in cell growth. The synthetic lethality produced by the combination of *tpm2Δ* and *tpm1Δ* was verified by showing that eleven haploid double mutants analyzed all required the presence of either the *TPM1* or *TPM2* gene on a plasmid for viability. This demonstrates that tropomyosins are required for some essential function in *S. cerevisiae*, although the loss of either gene product alone is tolerated.

Tpm2p Over-expression Alters Haploid Budding Pattern

To gain insight into the function of Tpm2p, the *GAL1-TPM2*

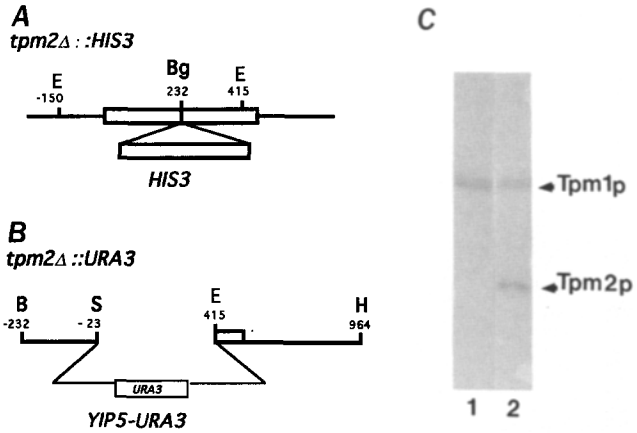

Figure 5. Disruption of *TPM2*. (*A*) *tpm2Δ::HIS3* construct in pBD103 vector. The *HIS3* marker gene was inserted at the BglII site at position 232, disrupting the gene. (*B*) *tpm2Δ::URA3* construct in pBD104 vector. Disruption with this construct deletes all but the last 68 bases of COOH-terminal coding region. (*C*) Immunoblot using polyclonal antiserum raised against Tpm2p, which cross-reacts with Tpm1p. Lane *1*, heat stable soluble proteins from *tpm2Δ::HIS3* haploids (ABY436); and lane *2*, heat stable soluble proteins from wild type haploids (ABY440).

multicopy plasmid was introduced into haploid wild type cells. Galactose-induced over-expression of Tpm2p produced no obvious effects on the actin cytoskeleton (not shown), but did affect cell polarity (Fig. 6). Normally, haploid yeast cells exhibit an axial budding pattern, in which the new bud emerges adjacent to the chitinous bud scar left behind from the previous cell division. A bipolar pattern, in which bud emergence may occur adjacent to or at the opposite pole from the previous cell division, is typical of diploid cells (reviewed by Drubin, 1991; Madden et al., 1992). Approximately 40% of haploid cells overexpressing Tpm2p showed a shift from the axial budding pattern typical of haploid yeast cells (Fig. 6 *B*) to a bipolar budding pattern (Fig. 6 *C*). This effect was not seen when Tpm1p was expressed to similar levels using a *GAL1-TPM1* fusion on a multicopy plasmid. In haploid cells overexpressing both Tpm1p and Tpm2p, the degree of bipolar budding seen is 11%. This suggests that the effect on cell polarity seen in response to Tpm2p overexpression is a result of an altered ratio of Tpm2p and Tpm1p, in which Tpm2p is in excess. When Tpm1p production is raised to similar levels, the effect on cell polarity is reduced.

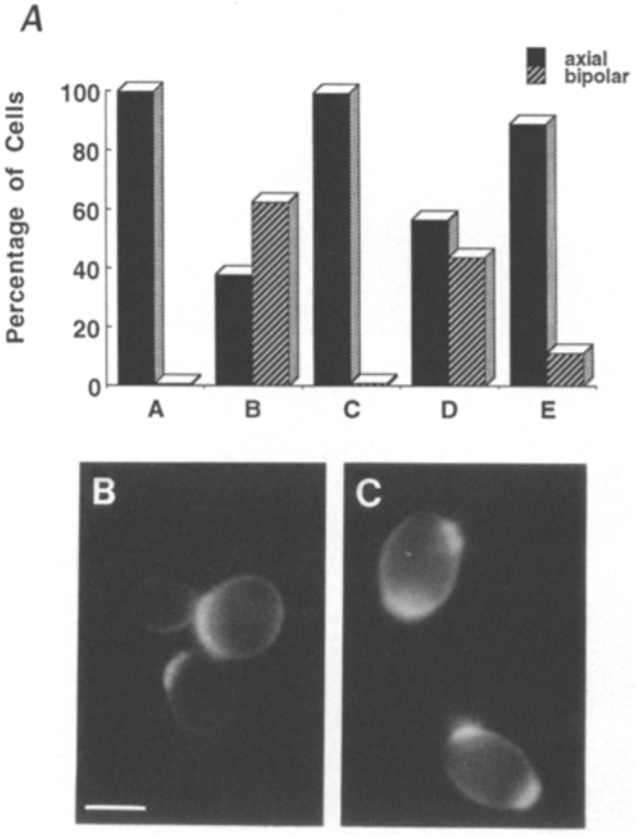

Figure 6. Effect of Tpm2p over-expression on budding pattern. (Panel *A*) Percentage of cells showing axial and bipolar budding. (*A*) Wild type haploids (CUY29); (*B*) wild type diploids (ABY173); (*C*) *GAL1-TPM1* over-expression haploids (ABY433) grown in galactose; (*D*) *GAL-TPM2* over-expression haploids grown in galactose (ABY431); (*E*) haploids overexpressing both *TPM1* and *TPM2* grown in galactose (*ABY434*). Cells were grown to log phase, labeled with Calcofluor, and cells with three or more bud scars were scored for axial or bipolar budding. (Panel *B*) Chitin labeling of wild type haploids (CUY29); (panel *C*) chitin labeling of haploids over-expressing *TPM2* (ABY431). Bar, 5 μm.

Over-expression of Tpm2p in tpm1Δ Cells Does Not Restore Wild Type Morphology

Disruption of the *TPM1* gene results in the disappearance of actin cables from the yeast cytoskeleton and random distribution of actin patches throughout both the mother and daughter cells (Fig. 7 *C*). Cells are defective in growth, mating projection formation, and cell fusion during mating. Chitin, which is normally limited to the septum which forms during budding, is often randomly deposited over the entire cell surface (Fig. 6 *D*). These problems are believed to be a result of a partial defect in the targeted delivery of components to the cell surface (Liu and Bretscher, 1992).

Galactose-induced over-expression of Tpm2p in a *tpm1Δ* strain (as shown in Fig. 2) resulted in partial restoration of actin cables in some cells (Fig. 7 *E*). In most cases, however, cells still showed an altered morphology and randomly distributed actin patches in both mother and bud. Overexpression of Tpm2p did not correct the defect in chitin localization in the *tpm1Δ* strain, indicating that the cells are still defective in targeted delivery to the cell surface. (Fig. 7 *F*). Since the level of expression of Tpm2p in these cells was significantly higher than the normal level of Tpm1p in wild type cells (not shown), these results demonstrate that Tpm2p cannot substitute functionally for Tpm1p, even when it is present at many times its normal level in the cell. Overexpression of Tpm1p to about the same level in *tpm1Δ* cells, restores fully the wild type phenotype (Liu and Bretscher, 1989b). These data indicate that Tpm2p cannot fully substitute for Tpm1p and is therefore functionally distinct.

Discussion

Vertebrates contain an amazing diversity of tropomyosin isoforms. They differ in expression level, tissue distribution, and intracellular localization as well as in their F-actin–binding properties and in the proteins with which they interact. Two size classes of tropomyosins have been recognized in vertebrates. Muscle tropomyosins contain 284 residues and span seven actin subunits along the actin filament. Smaller tropomyosins, having 247 or 248 residues, are the major forms found in non-muscle tissues and span six actin subunits in a filament. Within these size classes are isoforms that are tailor-made for specific functions. For example, splicing of the rat β-tropomyosin transcript in striated muscle cells results in a 284-residue protein with a domain containing a troponin-binding site, whereas alternative splicing of the same transcript in fibroblasts results in a 284-residue tropomyosin precisely lacking this domain (Helfman et al., 1986). The function of most vertebrate tropomyosin isoforms is not yet known. In this report we show that tropomyosin diversity extends to the yeast *S. cerevisiae*, in which two tropomyosin genes, *TPM1* and *TPM2*, encode proteins with distinct yet overlapping functions.

The product of the *TPM1* gene is the major tropomyosin in yeast and associates with actin filaments in vitro and in vivo (Liu and Bretscher, 1989*a*, *b*). Although the Tpm1p protein migrates in SDS gels with a mobility characteristic of the tropomyosins with 248 residues, analysis of the *TPM1* gene reveals a protein product with 199 residues. The prod-

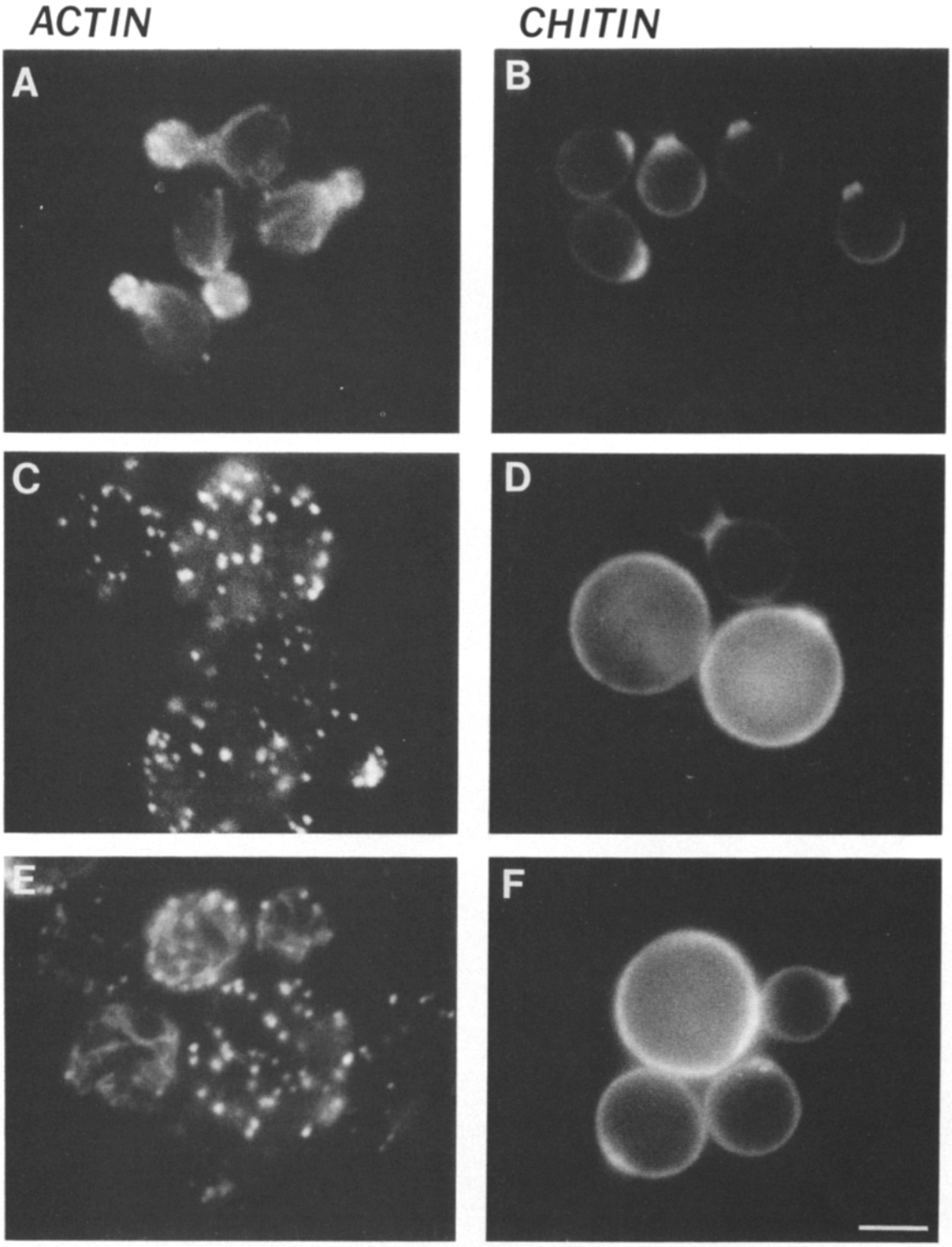

Figure 7. Actin (*A*, *C*, and *E*) and Chitin (*B*, *D*, and *F*) distribution in CUY29 wild type haploids (*A* and *B*); ABY167 *tpm1*Δ haploids (*C* and *D*); and ABY432 *tpm1*Δ haploids overexpressing *TPM2* and grown in galactose. Cells were grown to log phase, fixed, and treated with rhodamine–phalloidin to label F-actin and Calcofluor to label chitin. All panels are printed at the same final magnification. Bar, 5 μm.

uct of the *TPM2* gene described in this report is shorter still; it has only 161 residues. A diagram of the sequence relationships between the major classes of vertebrate tropomyosins with the yeast proteins is shown in Fig. 8. The two *S. cerevisiae* proteins show about 20% sequence identity to vertebrate tropomyosins, but are 64.5% identical to each other. This relatedness is supported by our biochemical studies; as is the case for Tpm1p, biochemical characterization establishes that Tpm2p is a tropomyosin with many features common to tropomyosins in other organisms. The fission yeast

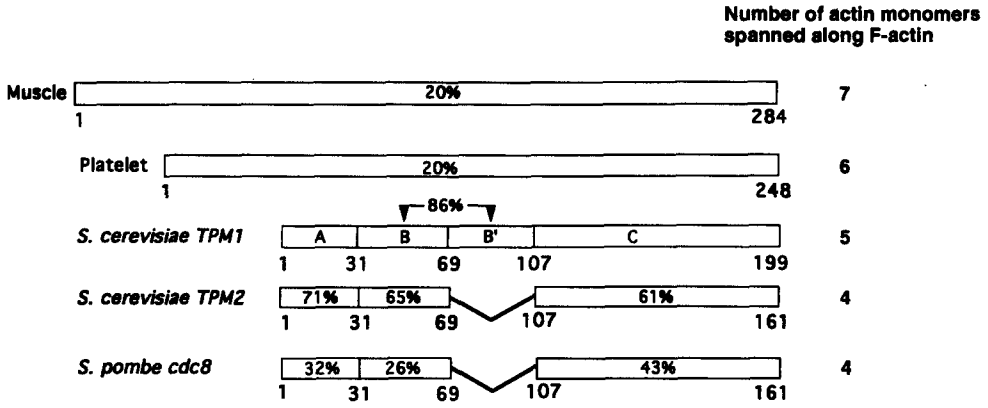

Figure 8. Diagram of the sequence relationships between vertebrate and yeast tropomyosins. The degree of overall sequence identity of vertebrate tropomyosins to Tpm1p is shown. Tpm1p has been divided into four regions: *A*, *B*, *B'*, *C*, with the *B* and *B'* regions representing the 38-amino acid pseudorepeats. The identity between the individual regions in Tpm1p to the *TPM2* and *cdc8* gene products is shown. The number of actin monomers spanned along F-actin has been determined experimentally (Cote, 1983; and this study) with the exception of the *S. pombe* protein, which is suggested by homology with Tpm2p.

Schizosaccharomyces pombe is another example of a primitive eukaryote which has at least two tropomyosin isoforms, a higher molecular weight protein which is immunologically related to Tpm1p (Liu and Bretscher, 1989*a*) and a lower molecular weight form of identical size to Tpm1p, encoded by *cdc8*, which is essential for cytokinesis (Balasubraminian et al., 1992).

Could there be additional tropomyosins in *S. cerevisiae*? Tpm1p is clearly the major isoform, and the only other one we have detected is Tpm2p, which is present at about one sixth the abundance of Tpm1p. If there are additional isoforms, they must be much less abundant than Tpm2p, so the presence of additional forms cannot be completely excluded. Moreover, tropomyosins, present only at specific stages of the yeast life cycle, such as during mating or sporulation, would not have been identified in our studies.

The 284-residue muscle tropomyosins make seven half-turns per molecule and span seven actin monomers as they lie in the grooves along either side of the actin filament (Philips et al., 1986). Each half-turn comprises approximately 39 residues of the α helix, with additional residues at the ends of the protein for head-to-tail overlap between adjacently bound tropomyosins. Disruption of the structural periodicity by removal of part of a half-turn disrupts actin-binding ability (Hitchcock-DeGregori and Varnell, 1990). The shorter 247- or 248-residue non-muscle tropomyosins span six actin monomers along the filament as determined biochemically and using this estimate of actin binding site size (Cote, 1983). Assuming that Tpm1p and Tpm2p follow the same structural rules as vertebrate tropomyosins, the number of actin monomers that each protein is predicted to span is five and four, respectively (Fig. 8). Measurements of the ratio of tropomyosin bound to F-actin under saturating conditions show that the molar ratio of actin monomers to Tpm1p dimers is about 4.6, and of actin monomers to Tpm2p dimers 3.6. These values are in good agreement with the predicted values.

Analysis of the Tpm1p sequence reveals that it has a 38 amino acid pseudorepeat, with the two sequences being 85% identical (Fig. 8). Tpm2p precisely lacks one of these repeats. Vertebrate tropomyosins do not show such obvious pseudorepeating regions; they must be a feature of primitive tropomyosins which was not conserved throughout evolution. In light of the size of this repeat, and the number of actins that Tpm1p and Tpm2p span along a filament, the repeat is strongly suggestive of an actin monomer binding site.

We have used a number of approaches to try to elucidate the similarities and differences in properties and functions of Tpm1p and Tpm2p. In vitro studies reveal that the profile of Mg^{2+}-dependent binding of Tpm2p to F-actin is very similar to that of Tpm1p and vertebrate non-muscle tropomyosins. As expected, binding of Tpm2p to F-actin decreases with increasing ionic strength, but in a manner quite distinct from that seen with Tpm1p (Liu and Bretscher, 1989*a*). The binding of Tpm1p to F-actin is very sensitive to the salt concentration, being nearly abolished at 300 mM KCl. In contrast, Tpm2p binding is reduced by less than 50% at 400 mM KCl under otherwise identical conditions. Under conditions optimal for binding of both tropomyosins, Tpm1p and Tpm2p can influence each others' actin binding behavior, which establishes that they can inhabit the same actin filament. Competition studies reveal that Tpm2p can compete with and decrease Tpm1p's binding to F-actin in vitro. Since Tpm2p appears to have four F-actin-binding sites, compared with Tpm1p's five, these four sites must bind F-actin with a higher affinity or there must be more head-to-tail interaction between Tpm2p molecules to achieve this effect. Since there appears to be sufficient Tpm1p protein in vivo to bind to all available F-actin (Liu and Bretscher, 1989*a*), it is not surprising that the much less abundant Tpm2p binds F-actin more tightly than Tpm1p, otherwise little of it would bind F-actin in vivo.

Changes in tropomyosin expression accompany changes in morphology in cultured cells transformed by oncogenic viruses, such as SV-40 and the Rous sarcoma virus (Cooper et al., 1985; Lin et al., 1985). Microfilament content of the major nonmuscle tropomyosins is decreased, while the content of the minor isoforms increases. This altered balance of

tropomyosin expression is likely to be involved with or to be a direct cause of the cytoskeletal changes typical of transformed cells (Matsumara et al, 1983; Lin et al., 1985). We found that altering the relative expression levels of Tpm1p and Tpm2p in yeast has an effect on cell polarity, specifically on bud site selection. Over-expression of Tpm2p, but not of Tpm1p, resulted in a shift from axial to bipolar budding in haploid cells. Since this effect can be partially suppressed by over-expression of Tpm1p, the ratio of the two tropomyosins appears to be important for correct morphogenesis. Thus, inappropriate replacement of Tpm1p by Tpm2p alters microfilament composition, which in turn alters determination of cell polarity.

Disruption of *TPM2* reveals that, like *TPM1*, it is not an essential gene. *tpm1Δ* cells are sickly and have multiple defects in growth and targeting of components to the cell surface (Liu and Bretscher, 1989*b*, 1992); *tpm2Δ* cells have no detectable phenotype. Combination of these two disruptions results in lethality, demonstrating that tropomyosins are required for some essential function in yeast. The two tropomyosins may act together in this function, or they may simply share enough structural and functional similarity to allow each one to compensate for the other's absence and thereby maintain viability.

While genetic evidence indicates that Tpm1p and Tpm2p function together or cooperate in some way, in vitro studies show that the proteins are biochemically distinct. In addition, *TPM1* interacts genetically with *MYO2* (Liu and Bretscher, 1992), whereas *TPM2* appears to have no such interaction. The failure of Tpm2p overexpression to rescue the cytoskeletal or transport defects in the *tpm1Δ* mutant provides in vivo evidence for functional differences. Therefore, while the two proteins are clearly able to participate in the performance of some essential cellular function, Tpm1p and Tpm2p are not functionally identical. We believe that each is involved in additional, distinct cellular processes. Identification of those gene products which interact with both Tpm1p and Tpm2p and those which interact specifically with only one of them should illuminate the nature of their functional divergence.

We thank members of the yeast cytoskeleton community for supplying us with strains, including A. Adams, D. Botstein, S. Brown, D. Drubin, T. Huffaker, G. Johnston, S. Lillie, and E. Orr.

This work was supported by PHS grant GM36552.

Received for publication 13 September 1994 and in revised form 8 November 1994.

References

Adams, A. E. M, D. Botstein, and D. G. Drubin. 1991. Requirement of yeast fimbrin for actin organization and morphogenesis in vivo. *Nature (Lond.).* 354:404–408.

Balasubraminiam, M. K., D. M. Helfman, and S. M. Hemmingsen. 1992. A new tropomyosin essential for cytokinesis in the fission yeast *Schizosaccharomyces pombe. Nature (Lond.).* 360:84–87.

Breitbart, R. E., A. Andreadis, and B. Nadal-Ginard. 1987. Alternative splicing: a ubiquitous mechanism for the generation of multiple protein isoforms from single genes. *Ann. Rev. Biochem.* 56:467–495.

Bretscher, A. 1984. Smooth muscle caldesmon: rapid purification and F-actin cross-linking properties. *J. Biol. Chem.* 259:12873–12880.

Bretscher, A. 1986. Thin filament regulatory proteins of smooth and nonmuscle cells. *Nature (Lond.).* 321:726–727.

Bretscher, A. P., B. Drees, E. Harsay, D. Schott, and T. Wang. 1994. What are the basic functions of microfilaments? Insights from studies in budding yeast. *J. Cell Biol.* 126:821–825.

Broschat, K. O., and D. R. Burgess. 1986. Low M^r tropomyosin isoforms from chicken brain and intestinal epithelium have distinct actin-binding properties. *J. Biol. Chem.* 261:13350–13359.

Cooper, H. L., N. Feuerstein, M. Noda, and R. H. Bassin. 1985. Suppression of tropomyosin synthesis, a common biochemical feature of oncogenesis by structurally diverse retroviral oncogenes. *Mol. Cell. Biol.* 5:972–983.

Cote, G. P. 1983. Structural and functional properties of the non-muscle tropomyosins. *Mol. Cell. Biochem.* 57:127–146.

Cote, G. P., and L. B. Smillie. 1981*a*. Preparation and some properties of equine platelet tropomyosin. *J. Biol. Chem.* 256:11004–11010.

Cote, G. P., and L. B. Smillie. 1981*b*. The interaction of equine platelet tropomyosin with skeletal muscle actin. *J. Biol. Chem.* 256:7257–7261.

Drubin, D. G. 1991. Development of cell polarity in budding yeast. *Cell.* 65:1093–1096.

Drubin, D. G., K. G. Miller, and D. Botstein. 1988. Yeast actin binding proteins: evidence for a role in morphogenesis. *J. Cell Biol.* 107:2551–2561.

Ebashi, S., I. Ohtsuki, and K. Mihashi. 1972. *Cold Spring Harbor Symp. Quant. Biol.* 37:215–223.

Fowler, V. M., and V. Bennett. 1984. Erythrocyte membrane tropomyosin, purification and properties. *J. Biol. Chem.* 259:5978–5989.

Goff, C. G., D. T. Moir, T. Kohno, T. C. Gravius, R. A. Smith, E. Yamasaki, and A. Taunton-Rigby. 1984. Expression of calf prochymosin in *Saccharomyces cerevisiae. Gene.* 27:35–46.

Haarer, B. K., A. Petzold, S. Lillie, and S. S. Brown. 1994. Identification of *MYO4*, a second class V myosin gene in yeast. *J. Cell. Sci.* 107:1055–1064.

Helfman, D. M., S. Cheley, E. Kuismanen, L. A. Finn, and Y. Yamawaki-Kataoka. 1986. Nonmuscle and muscle tropomyosin isoforms are expressed from a single gene by alternative RNA splicing and polyadenylation. *Mol. Cell Biol.* 6:3582–3595.

Hendricks, M., and H. Weintraub. 1981. Tropomyosin is decreased in transformed cells. *Proc. Natl. Acad. Sci. USA.* 78:5633–5637.

Hill, J. E., A. M. Meyers, T. J. Koerner, and A. Tzagoloff. 1986. Yeast/*E. coli* shuttle vectors with multiple unique restriction sites. *Yeast.* 2:163–167.

Hitchcock-DeGregori, S. E., and T. A. Varnell. 1990. Tropomyosin has discrete actin-binding sites with sevenfold and fourteenfold periodicities. *J. Mol. Biol.* 214:885–896.

Ito, H., Y. Jukuda, K. Murata, and A. Kimura. 1983. Transformation of intact yeast cells treated with alkali cations. *J. Bacteriol.* 153:163–168.

Johnston, G. C., J. A. Prendergast, and R. A. Singer. 1991. The *S. cerevisiae MYO2* gene encodes an essential myosin for vectorial transport of vesicles. *J. Cell Biol.* 113:539–551.

Lin, J.J-C., D. M. Helfman, S. H. Hughes, and C.-S. Chou. 1985. Tropomyosin isoforms in chicken embryo fibroblasts: purification, characterization, and changes in Rous Sarcoma virus-transformed cells. *J. Cell Biol.* 100: 692–703.

Lin, J.J-C., T. E. Hegman, and J. L-C. Lin. 1988. Differential localization of tropomyosin isoforms in cultured nonmuscle cells. *J. Cell Biol.* 107: 563–572.

Liu, H., and A. Bretscher. 1989*a*. Purification of tropomyosin from *Saccharomyces cerevisiae* and identification of related proteins in *Schizosaccharomyces* and *Physarum. Proc. Natl. Acad. Sci. USA.* 86:90–93.

Liu, H., and A. Bretscher. 1989*b*. Disruption of the single tropomyosin gene in yeast results in the disappearance of actin cables from the cytoskeleton. *Cell.* 57:233–242.

Liu, H., and A. Bretscher. 1992. Characterization of *TPM1* disrupted yeast cells indicates an involvement of tropomyosin in directed vesicular transport. *J. Cell Biol.* 118:285–299.

Madden, K., C. Costigan, and M. Snyder. 1992. Cell polarity and morphogenesis in *Saccharomyces cerevisiae. Trends Cell Biol.* 2:22–29.

Matsumara, F., and S. Yamashiro-Matsumara. 1985. Purification and characterization of multiple isoforms of tropomyosin from rat cultured cells. *J. Biol. Chem.* 260:13851–13859.

Matsumara, F., J.J-C. Lin, S. Yamashiro-Matsumara, G. P. Thomas, and W. C. Topp. 1983. Differential expression of tropomyosin forms in the microfilaments isolated from normal and transformed rat cultured cells. *J. Biol. Chem.* 258:13954–13964.

Mulholland, J., D. Preuss, A. Moon, A. Wong, D. Drubin, and D. Botstein. 1994. Ultrastructure of the yeast actin cytoskeleton and its association with the plasma membrane. *J. Cell Biol.* 125:381–391.

Payne, M. R., and S. E. Rudnick. 1985. Tropomyosin, structural and functional diversity. *Cell Muscle Motil.* 6:141–184.

Philips, G. N., J. P. Fillers, and C. Cohen. 1986. Tropomyosin crystal structure and muscle regulation. *J. Mol. Biol.* 192:111–131.

Pittenger, M. F., and D. M. Helfman. 1992. In vitro and in vivo characterization of four fibroblast tropomyosins produced in bacteria:TM-2, TM-3, TM-5a, and TM-5b are co-localized in interphase fibroblasts. *J. Cell Biol.* 118:841–858.

Russel, D. W., R. Jensen, M. J. Zoller, J. Burke, B. Errede, M. Smith, and I. Herskowitz. 1986. Structure of the Saccharomyces cerevisiae HO gene and of its upstream regulatory region. *Mol. Cell Biol.* 6:4281.

Stewart, M. 1975. Tropomyosin: Evidence for no stagger between chains. *FEBS Lett.* 53:5–7.

Stone, D., and L. B. Smillie. 1978. The amino acid sequence of rabbit skeletal α-tropomyosin. *J. Biol. Chem.* 253:1137–1148.

Wang, R., and B. T. Chait. 1994. High accuracy mass measurement as a tool for studying proteins. *Curr. Opin. Biotechnol.* 5:77–84.

Watts, F. Z., G. Shiels, and E. Orr. 1987. The yeast *MYO1* gene encoding a myosin-like protein required for cell division. *EMBO (Eur. Mol. Biol. Organ.) J.* 6:3499–3505.

Welch, M. D., D. A. Holtzman, and D. G. Drubin. 1994. The Yeast Actin Cytoskeleton. *Curr. Opin. Cell Biol.* 6:110–119.